Journal Pre-proofs

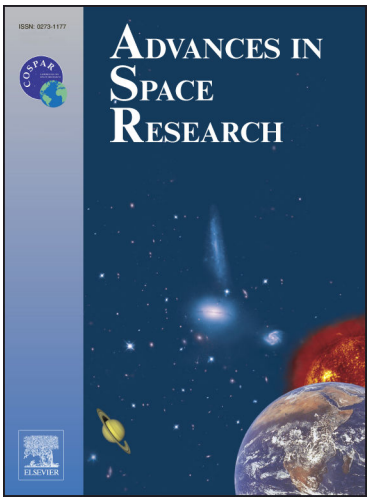

Performance of the IRI-2016 and IRI-Plas 2020 considering Mg II as EUV solar proxy

Blas F. de Haro Barbas, Bruno S. Zossi, Gloria Tan Jun, Manuel Bravo, Miguel Martinez-Ledesma, Valentin Venchiarutti, Gilda Gonzalez, Franco D. Medina, Trinidad Duran, Ana G. Elias

PII: S0273-1177(23)00437-4
DOI: https://doi.org/10.1016/j.asr.2023.06.007
Reference: JASR 16764

To appear in: *Advances in Space Research*

Received Date: 9 April 2023
Revised Date: 30 May 2023
Accepted Date: 5 June 2023

Please cite this article as: de Haro Barbas, B.F., Zossi, B.S., Tan Jun, G., Bravo, M., Martinez-Ledesma, M., Venchiarutti, V., Gonzalez, G., Medina, F.D., Duran, T., Elias, A.G., Performance of the IRI-2016 and IRI-Plas 2020 considering Mg II as EUV solar proxy, *Advances in Space Research* (2023), doi: https://doi.org/10.1016/j.asr.2023.06.007

This is a PDF file of an article that has undergone enhancements after acceptance, such as the addition of a cover page and metadata, and formatting for readability, but it is not yet the definitive version of record. This version will undergo additional copyediting, typesetting and review before it is published in its final form, but we are providing this version to give early visibility of the article. Please note that, during the production process, errors may be discovered which could affect the content, and all legal disclaimers that apply to the journal pertain.

© 2023 COSPAR. Published by Elsevier B.V. All rights reserved.

Performance of the IRI-2016 and IRI-Plas 2020 considering Mg II as EUV solar proxy

Blas F. de Haro Barbas[1], Bruno S. Zossi[1,2], Gloria Tan Jun[3], Manuel Bravo[4,5], Miguel Martinez-Ledesma[5,6], Valentin Venchiarutti[1], Gilda Gonzalez[1], Franco D. Medina[1,2], Trinidad Duran[7,8], Ana G. Elias[1,2]

1. LIANM, FACET, Universidad Nacional de Tucuman, Argentina
2. INFINOA, CONICET-UNT, Argentina
3. German Aerospace Center (DLR), Institute for Solar-Terrestrial Physics, Neustrelitz, Germany
4. Centro de Instrumentación Científica (CInC), Universidad Adventista de Chile, Chillán, Chile
5. Centro Interuniversitario de Física de la Alta Atmósfera (CInFAA), Chile
6. CePIA, Departamento de Astronomía, Universidad de Concepción, Concepción, Chile
7. Departamento de Física, Universidad Nacional del Sur (UNS), Bahía Blanca, Argentina
8. Instituto de Física del Sur (CONICET-UNS), Bahía Blanca, Argentina

Journal Pre-proofs

Abstract

To assess upper atmosphere parameters, current models use different variables to account for solar activity levels. Studies that evaluate the most recent solar cycles have shown that when dealing with the ionospheric F2 layer, and in particular with foF2, the Mg II index is a better choice than other solar activity proxies to account for solar EUV variation. The International Reference Ionosphere, version 2016 (IRI-2016), a model widely used by the scientific community, uses the Ionosonde Global (IG) index to assess foF2. A most recent and expanded version, IRI-Plas, allows selecting a solar activity proxy among 7 options including IG and Mg II. In the present work, the performance of IRI considering Mg II to assess foF2 is analyzed, comparing three modeling cases: IRI-2016 with its default solar activity index (IG), IRI-2016 with Mg II instead of IG, and IRI-Plas choosing Mg II as the solar proxy option. This model comparison was evaluated in terms of their agreement with measured foF2 data from four stations located in Japan (Northern Hemisphere), and four in Australia (Southern Hemisphere). Monthly medians for the 24 hours, along two periods of three years were considered: 2000-2002 and 2008-2010, which correspond to epochs of maximum and minimum solar activity levels, respectively. Based on goodness-of-fit statistics, our results show that in the case of IRI-2016, the Mg II implementation does not reveal a significant improvement for foF2 assessment, and the IRI-Plas performance with the Mg II option is only slightly better than the other two options. Dispersion diagrams between measured and modeled foF2 also evince a similar performance between the three models. All models show the same over- and underestimation patterns, except in the nighttime case during the minimum activity level period for both Australian and Japanese stations where IRI-Plas outperforms the other two model options. The comparable performances of the three options might be attributed to a stronger variation in the evaluated periods which could be related to seasonal changes rather than to solar EUV proxies. Future studies

considering time series over several years, covering at least a complete solar activity cycle, are required to determine stronger model performance differences.

Keywords: International Reference Ionosphere, solar activity proxies, Mg II index, foF2, comparative analysis

Highlights:

- Mg II index was implemented in IRI-2016 to assess foF2 but results do not provide a clear improvement of the model performance
- IRI-Plas with Mg II option to assess foF2 provides a slightly better performance than IRI-2016

1. Introduction

The Sun is the main source of energy for our planet, thus having a direct impact on the structure of our atmosphere. Therefore, to determine the behavior of the different atmospheric layers, in particular the upper atmosphere, it is essential to analyze the influence of solar activity variability. Depending on the radiation spectral range of interest, different solar activity proxies have been commonly used in the literature to consider the impact of solar variations on the atmosphere. The variations of the solar EUV radiation flux, which are directly linked to solar activity changes, are the main responsible for the variability of the different ionospheric layers. Indeed, recent studies have demonstrated that the usage of different indices to measure the solar EUV does not always provide the same ionospheric reproducibility accuracy (Lastovicka, 2021a, 2021b; Danilov and Konstantinova, 2023).

Unfortunately, long-term measurements of solar EUV fluxes spanning several decades are not readily accessible. As a result, researchers rely on different solar activity proxies when studying the ionosphere over extended periods. These indices are essential for investigating climatology, long-term trends, and changes in space climate. They provide valuable information for understanding the effects of solar activity on the ionosphere despite the lack of direct long-term EUV measurements.

Early works linking ionospheric parameters with solar activity variations used the sunspot number, Rz, as a proxy. Actually, Rz is the solar activity proxy with the longest record, dating back to 1749 on a monthly basis, and to 1700 on a yearly basis (Clette et al., 2014). This index, together with the 10.7 cm solar flux, F10.7, have been traditionally used in ionospheric studies (Liu et al., 2011). Nevertheless, several long-term trend studies have evidenced that F10.7 is a better proxy than Rz in representing solar EUV flux for ionospheric research (Lastovicka et al., 2006; Mielich and Bremer, 2013; Deminov et al., 2020). Furthermore, recent studies recommend the use of the Mg II index (core-to-wing ratio derived from the Mg II doublet at 280 nm) as a solar proxy for F2-layer critical frequency, foF2 (Lastovicka 2021a, 2021b), while F10.7 is still recommended for E-layer critical frequency, foE and Total Electron Content, TEC (Lastovicka, 2021a).

The International Reference Ionosphere (IRI) is an empirical model of the ionosphere that uses data from a worldwide network of several instruments (such as ionosondes, satellites, rockets, etc.) and became an official standard model with a very large user community (Bilitza et al., 2017, 2022). To model the variability of the critical frequency of the F2 layer, foF2, related to the solar activity, IRI uses the Ionosonde Global (IG) index (Liu et al., 1983). This index was originally based on 11 reference stations, but currently

it is determined with only four (two from the Southern Hemisphere and two from the Northern Hemisphere). Even though this small number of ionosondes has limited the reliability of the IG index in representing global ionospheric conditions, according to Bilitza et al. (2022) it describes the solar cycle changes in foF2 better than Rz and F10.7, since it is obtained from ionospheric measurements and may include dynamic effects not covered by solar indices. The IRI model has continuously been updated thanks to the effort of a big community of researchers around the world. This model calculates several ionospheric parameters such as the ion concentration, electron density, temperature, vertical drift, among others. Nevertheless, even the latest version of this model, IRI-2020, still considers IG for foF2 assessments.

On the other hand, there is an IRI adaptation, the IRI-Plas 2020 version, that has been modified to model also the plasmasphere extending up to 20,000 km (Gulyaeva et al., 2011). This model has been used for different applications such as high frequency (HF) signal studies (Sezen et al., 2013; Erdem and Arikan, 2017), or computed ionospheric tomography (Tuna et al., 2014; Erturk et al. al., 2009). Moreover, the IRI-Plas model allows selecting between different solar proxies to estimate foF2, and among them the Mg II index.

The evaluation of IRI model performance is a relevant area of study, as there is a continuous need to recalculate its fittings over time due to the constant addition of new measured data. Moreover, there are many studies which analyze the agreement between IRI modeled and observed foF2, but very few studies make a comparison among the performance of different IRI options. Many comparisons are made considering hourly values, and even with minute resolution, which would explain the errors magnitude being on average ~1-1.5 MHz (Maltseva and Poltavsky, 2009; Arikan et al., 2019). Nevertheless, when monthly medians are considered, the mean error falls to ~0.5 MHz (Maltseva and Poltavsky, 2009; Tsagouri et al., 2018; Liu et al., 2019).

Previous studies have already analyzed if the degree of agreement of the IRI model can be further improved by considering Mg II as the solar activity index. These studies have been done using IRI-Plas, but mainly focusing on the accuracy of TEC. The study of Sezen et al. (2018) is the first work to compare ionosonde foF2 data to IRI-Plas foF2 values using all the solar proxy options available in this model but considering daily mean values. In their study, the best fitting in terms of root mean squared error (RMSE) is obtained, for the mid-latitude ionosphere, with the Lyman α solar proxy followed by IG and Mg II solar proxies. Additionally, the study of Abbas and Ameen (2022) evaluated the IRI-Plas ability to model foF2 considering four different proxies: F10.7, IG, Mg-II, and Lyman-α. Their results show that IRI-Plas model using Mg-II proxy option generally performed better than with the other options, being Lyman-α the worst, in contrast to the results of Sezen et al. (2018). Nevertheless, these studies are based on the comparison of daily mean values, providing a RMSE difference between each proxy performance of around 0.5 MHz, which accounts for the monthly median RMSE value previously indicated.

In this study, we evaluate the performance of IRI to model foF2 using Mg II as a solar EUV proxy, in comparison to the traditional IG index. As the IRI modeled foF2 provides a better agreement with foF2 measurements on monthly timescales, our evaluation is carried out through a direct comparison with foF2 observations based on monthly medians. Moreover, two IRI versions are considered: IRI-2016 and IRI-Plas. The first one is still widely used by the community thanks to its wide accessibility, so we implemented the Mg II index in it by scaling the Mg II to IG metrics. In the case of IRI-Plas, the Mg II index option to assess foF2 was selected in the running process. A quantitative evaluation for eight selected ionospheric stations is provided that can be of significance for users and developers of this fundamental ionospheric model. The results of this study aim to provide a better IRI modeling tool for long-term solar variation studies.

2. Data and Methodology

In order to analyze IRI performance to model foF2 using Mg II as a solar EUV proxy in comparison to the traditional IG index, a statistical comparative analysis was carried out between modeled and measured foF2 values. In the modeled case, three options that are described below were considered in order to assess the convenience of using Mg II as the solar proxy to model foF2 on a monthly basis.

2.1. foF2 measured data

Monthly median foF2 data from eight mid-latitude stations (four from Japan and four from Australia), listed in Table 1, were used for this comparative analysis. Japanese stations data was obtained from https://wdc.nict.go.jp/IONO/ and in the Australian case from https://sws.bom.gov.au/World_Data_Centre/1/3. These stations were selected based on IRI reliability to reproduce mid-latitude ionosphere and the long dataset availability. Two of these stations (Kokubunji and Canberra) are currently used in the IG calculation of IRI (Brown et al., 2018). Monthly median data assessed from fewer than 15 daily data were removed from the corresponding foF2 time series.

The ionosonde dataset consists of 24-hour values for two periods of three years each: 2000-2002 and 2008-2010, which correspond to maximum and minimum solar activity levels, respectively. These two periods were chosen expecting to find greater differences between solar proxies. Correlation coefficients between any pair of solar activity proxies for periods covering a complete solar cycle, or more, are greater than 0.95. However, when we focus on shorter periods, the coefficients decrease, specifically during maximum and minimum epochs (Bruevich et al., 2014; Elias et al., 2021). This may be because the variation linked to the quasi-decadal cycle is minimal at these levels of activity (first derivatives are zero since we are at a maximum or minimum of the curves). Hence, the time variation due to specific forcings of each proxy gains relative importance.

Table 1. Selected Japanese and Australian ionospheric stations. Latitude and Longitude correspond to geographic coordinates.

	Latitude	**Longitude**
Wakkanai	45.16 °N	141.75 °E
Kokubunji	35.71 °N	139.49 °E

Journal Pre-proofs

Yamagawa	31.20 °N	130.62 °E
Okinawa	26.68 °N	128.15 °E
Canberra	35.17 °S	149.19 °E
Brisbane	27.28 °S	153.02 °E
Hobart	42.53 °S	147.19 °E
Townsville	19.16 °S	146.48 °E

Journal Pre-proofs

2.2. IRI modeled foF2

Monthly median foF2 data was modeled from 0 to 23 LT for the two periods of three years considering two IRI versions: IRI-2016 and IRI-Plas.

The IRI-2016 model (Bilitza et al., 2017, 2022), freely available in Fortran source code at https://irimodel.org/IRI-2016/, is used to obtain foF2. As previously indicated, this model runs considering the IG index as a solar EUV proxy to assess foF2. To implement Mg II, this index was scaled to IG through a linear regression and then the original IG database was accordingly modified. The Mg II index used to scale IG was obtained from the University of Bremen and is freely available at http://www.iup.uni-bremen.de/UVSAT/Datasets/MgII (Viereck et al., 2010; Snow et al., 2014), covering the period November 1978-present. Fig. 1 shows IG12 (IG 12-month running mean) and Mg II, together with the corresponding dispersion diagram and its estimated linear regression fit. Therefore, modeled foF2 values were obtained with the traditional IRI-2016, which we called IRI, and with the modified version considering Mg II instead of IG, which we called IRImod.

The IRI-Plas model used was obtained from its online version available at www.ionolab.org. This model offers the possibility of selecting between nine solar proxies, among which is Mg II (Gulyaeva et al., 2017, 2018). In this case, the foF2 modeled values were obtained by selecting Mg II as the solar proxy to estimate this ionospheric parameter. In both models, IRI-2016 and IRI-Plas, daily values were obtained first for each hour and each station, followed by the monthly median calculation.

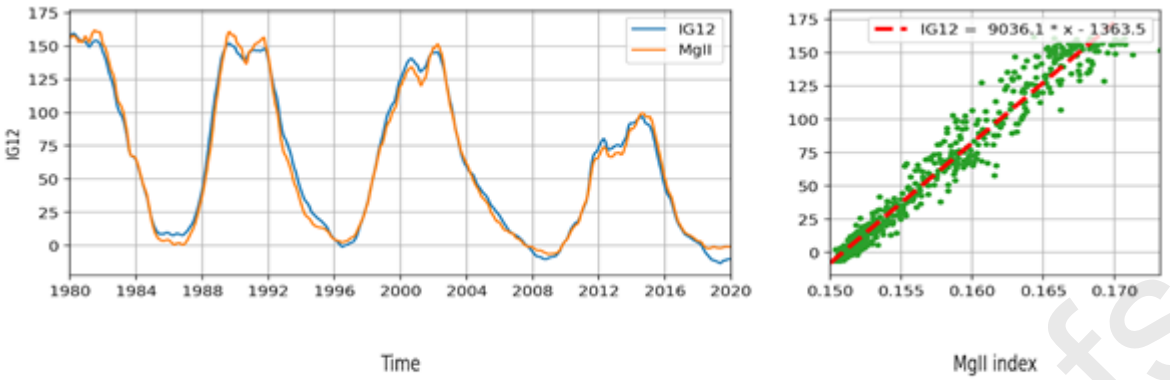

Figure 1. Left panel: Time variation of IG12 (blue) and scaled Mg II index (orange). Right panel: Dispersion diagram of IG12 vs. Mg II (green dots), and its linear regression fit (dashed red line).

2.3. Methodology

The monthly median foF2 data series of the three models, that is IRI, IRImod, and IRI-Plas, evaluated for each local time, from 0 to 23, were compared to foF2 observations. The following comparison metrics, commonly used in data-model prediction comparisons (e.g., Willmott and Matsuura, 2005; Chicco et al., 2021), were considered: Pearson's linear correlation coefficient (RHO), the mean relative error (MRE), and the mean absolute error (MAE), whose equations are listed in Table 2.

RHO measures the linear association strength between modeled and observed foF2, indicating how similar the variability of one series is to that of the other. It is bounded between 1 and -1, where 1 is the optimal value indicating that both time series vary identically. MRE measures the average bias of the modeled values over or underestimating the observed one depending on its sign: positive or negative, respectively. It gives similar information to the percentage bias, and its optimal value is 0. Finally, MAE is a scale-dependent measure of deviation that corresponds to the IRI model deviation from the observations. The optimal value of MAE is 0, indicating that both series are identical.

Considering that the time series compared cover three years of monthly data, that is 36 data points in total each, whenever the foF2 observed time series has less than 24 data points, the corresponding RHO, MAE and MRE were removed. Also, only the cases where RHO significance was higher than 95% were kept in this analysis.

Table 2. Equations for the statistical metrics to evaluate IRI, IRImod, and IRI-Plas performance. IRI models and observed foF2 data are represented by x and y, respectively; n corresponds to the number of points.

Name	Equation

Journal Pre-proofs

Pearson's correlation coefficient (RHO)	$RHO = \frac{n\,(\Sigma xy) - (\Sigma x)\,(\Sigma y)}{\sqrt{[n\Sigma x^2 - (\Sigma x)^2]\,[n\,\Sigma y^2 - (\Sigma y)^2]}}$
Mean relative error (MRE)	$MRE = \frac{1}{n}\Sigma\frac{(x-y)}{y}$
Mean absolute error (MAE)	$MAE = \frac{1}{n}\Sigma\lvert x-y\rvert$

3. Results

Figs. 2 and 3 show, as an example, monthly median foF2 values at noon for the selected stations during the low and high solar activity periods, 2008-2010 and 2000-2002 respectively, together with the corresponding IRI modeled values. It can be noticed that the main variation is due to seasonality. Japanese stations show a prevailing winter anomaly with a superposed semi-annual variation, and Australian stations exhibiting a dominant semi-annual variation with equinoctial maxima. The observed and modeled curves for each station and period appear to vary in phase.

Figs. 4 to 9 show the RHO, MAE, and MRE metrics calculated for each of the two periods, in terms of local time. The in-phase variation noticed in Figs. 2 and 3 is confirmed by the high RHO values for almost all the cases, as can be seen in Figs. 4 and 7. The exceptions occur during morning or late afternoon hours, where RHO drops below 0.7 in some cases during maximum solar activity level period, and to values lower than 0.5 during the minimum solar activity period. In the latter case, this occurs particularly during early morning hours. Regarding each model performance in terms of RHO, there is not any marked difference. Therefore, it can be said that they all reproduce the time variability in a monthly scale with a similar degree of agreement.

In the cases of MAE and MRE, the differences are relatively small, with the outperformance of each model alternating along hours and stations. However, some distinctions can be made. In the case of MAE (Figs. 5 and 8), during solar activity maximum, IRI-Plas performs considerably better in the case of Townsville and Okinawa. During the period of minimum solar activity, differences among the models are not so clear. This is also evidenced in the average values of MAE and MRE listed in Table 3, where MAE mean values are almost equal among the models for the 2008-2010 period.

Regarding MRE (Figs. 6 and 9), IRI-Plas is the better option during the maximum solar activity period. During the minimum solar activity epoch, IRI-Plas overestimates foF2 on average in the cases of Hobart, Townsville, Kokubunji, Okinawa and Yamagawa. This is supported by its mean value of 0.078 (see Table 3), which is one order of magnitude higher than MRE mean values for IRI and IRImod.

Overall, and based on Table 3, it could be said that IRImod and IRI-Plas, both using Mg II, are only slightly better than the version of IRI that uses IG.

Table 3. Mean MAE and MRE over the eight ionospheric stations and 24 hours, for each modeled foF2 (IRI, IRImod, and IRI-Plas) compared to foF2 observations, along each 3-year period (2000-2002 and 2008-2010).

	IRI	IRImod	IRI-Plas
MAE (2000-2002)	0.704	0.691	0.652
MAE (2008-2010)	0.524	0.526	0.546
MRE (2000-2002)	0.040	0.029	0.028
MRE (2008-2010)	-0.006	0.005	0.078

Journal Pre-proofs

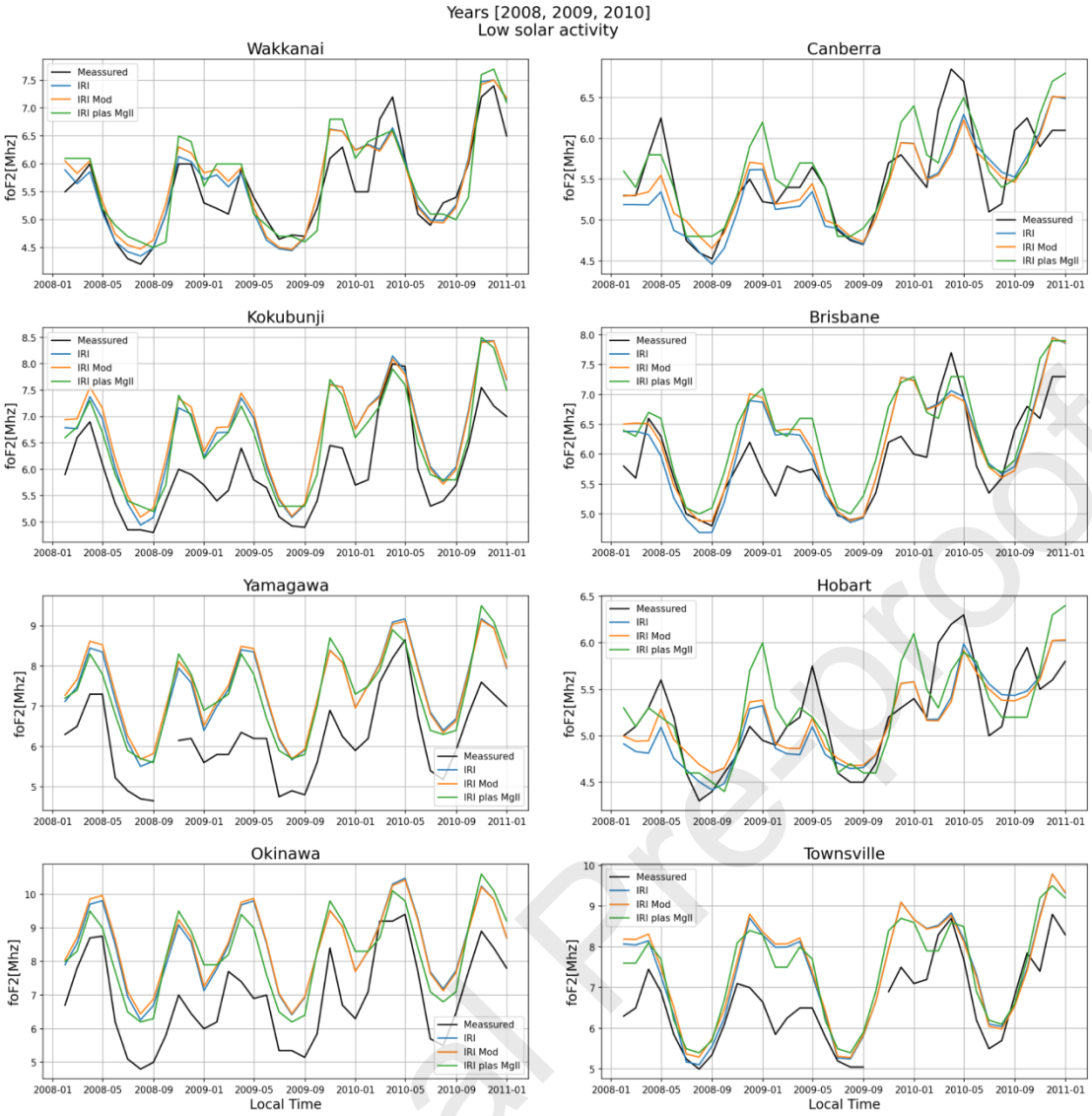

Figure 2. Noon monthly medians of foF2 for low solar activity years (2008-2010): measured (black line) and modeled foF2 with IRI (blue), IRImod (orange), and IRI-Plas (blue).

Journal Pre-proofs

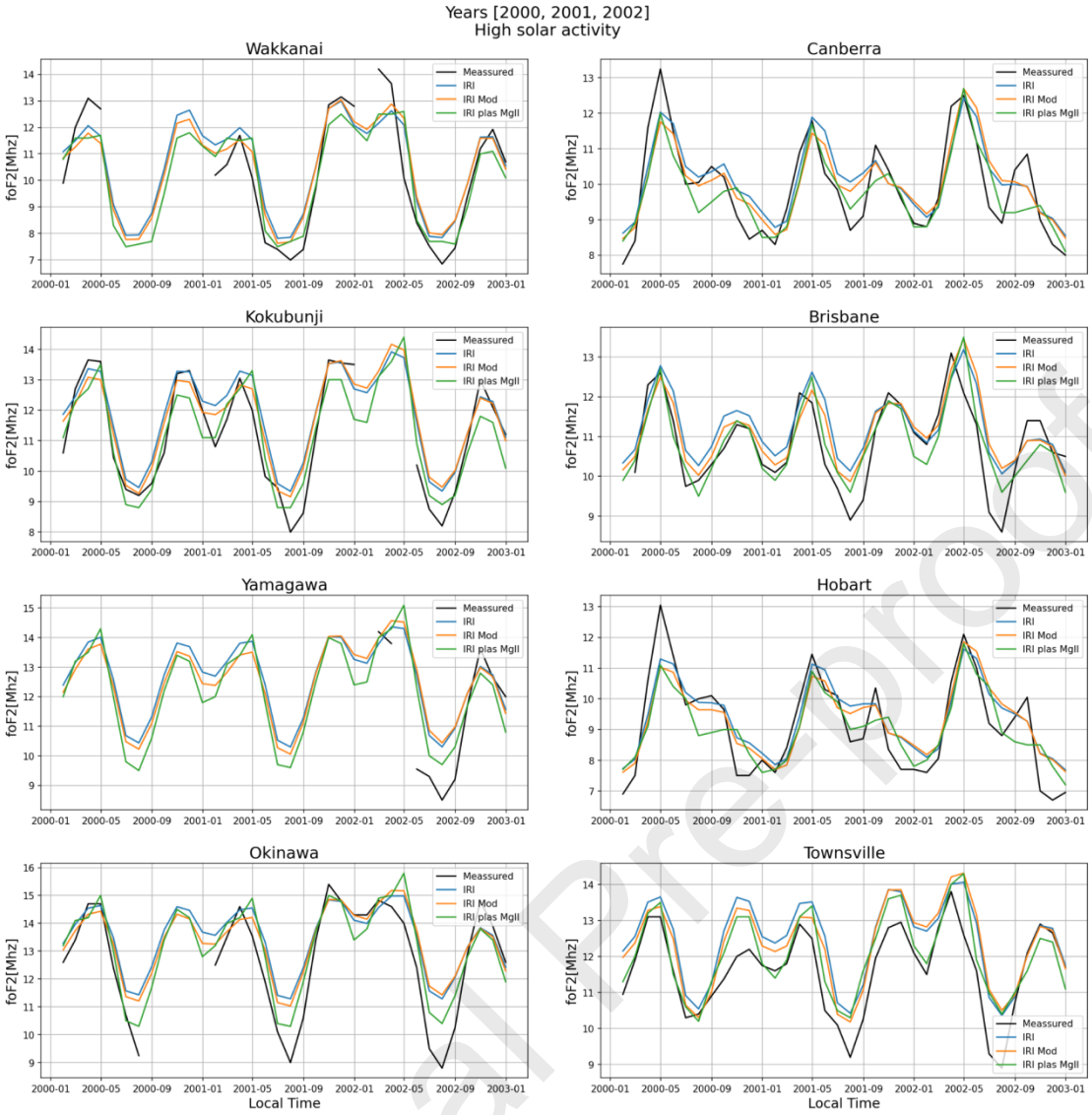

Figure 3. Noon monthly medians for high solar activity years (2000-2002): measured (black line) and modeled foF2 with IRI (blue), IRImod (orange), and IRI-Plas (blue).

Journal Pre-proofs

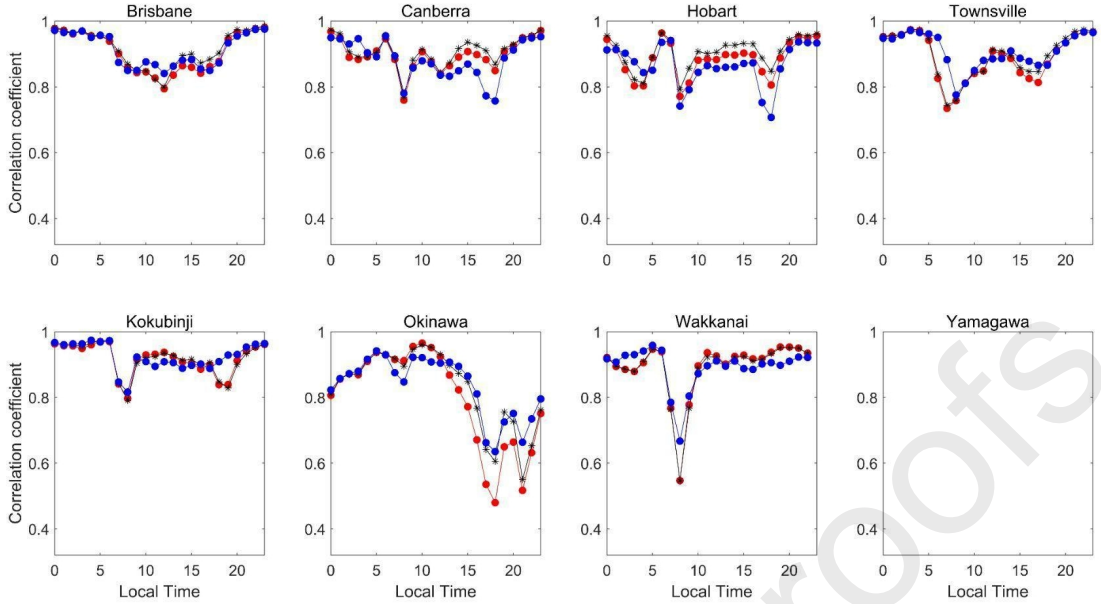

Figure 4. Correlation coefficient (RHO) between observed foF2 and modeled foF2 by: IRI (black asterisk), IRImod (red dots), and IRI-Plas using Mg II (blue dots) for each of the selected stations, in terms of local time. The correlated series consist of monthly medians covering the period January 2000-December 2002.

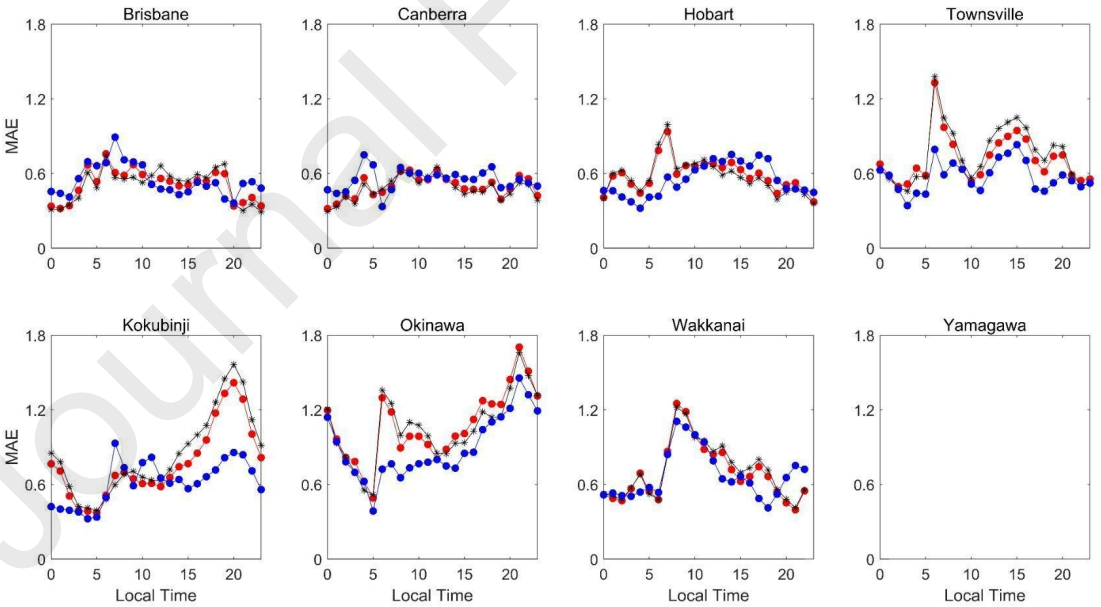

Figure 5. Mean Absolute Error (MAE) between observed foF2 and modeled foF2 by: IRI (black asterisk), IRImod (red dots), and IRI-Plas using Mg II (blue dots) for each of the selected stations, in terms of local time. The correlated series consist of monthly medians covering the period January 2000-December 2002.

Journal Pre-proofs

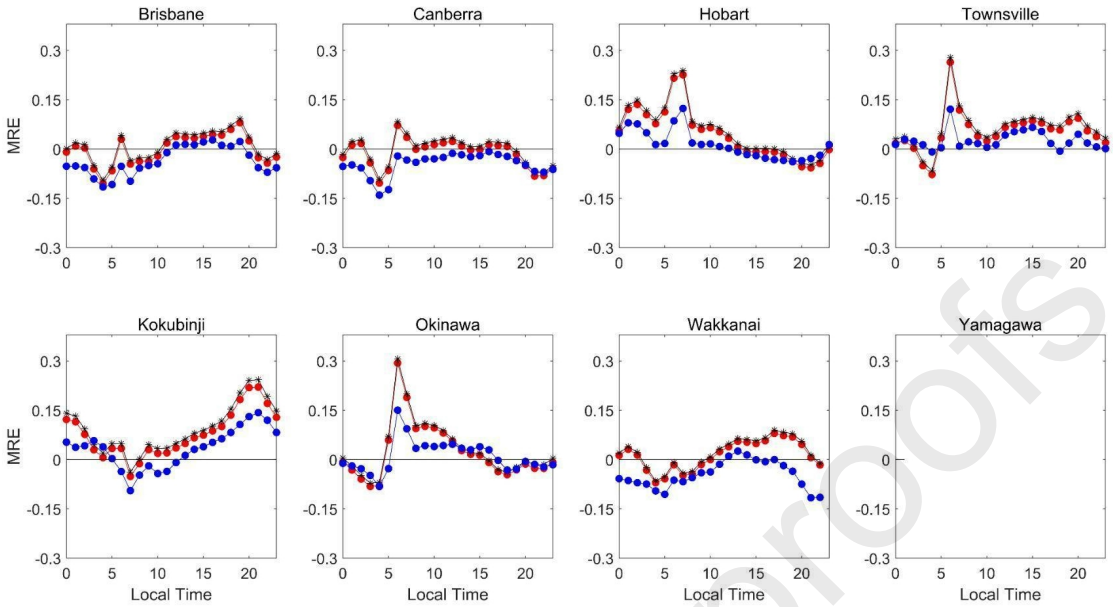

Figure 6. Mean Relative Error (MRE) between observed foF2 and modeled foF2 by: IRI (black asterisk), IRImod (red dots), and IRI-Plas using Mg II (blue dots) for each of the selected stations, in terms of local time. The correlated series consist of monthly medians covering the period January 2000-December 2002.

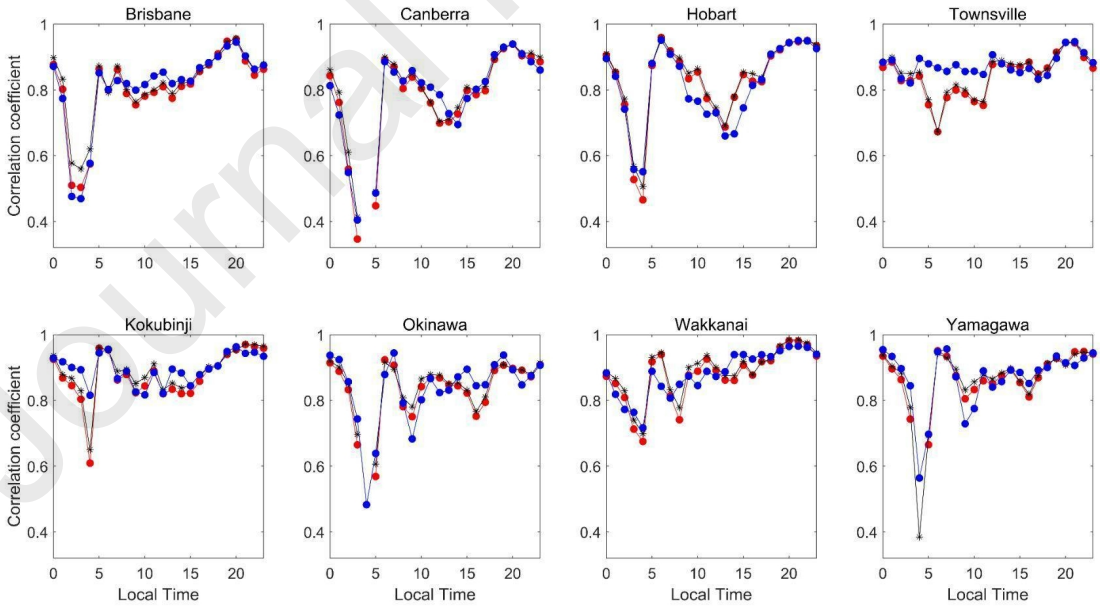

Figure 7. Correlation coefficient (RHO) between observed foF2 and modeled foF2 by: IRI (black asterisk), IRImod (red dots), and IRI-Plas using Mg II (blue dots) for each of the selected stations, in terms of local time. The correlated series consist of monthly medians covering the period January 2008-December 2010.

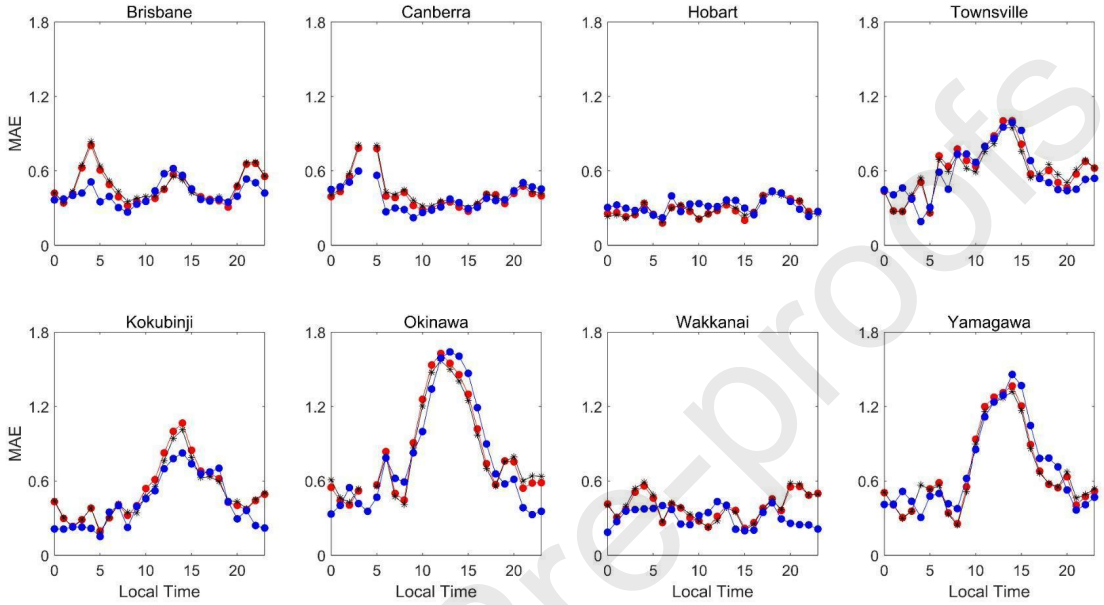

Figure 8. Mean Absolute Error (MAE) between observed foF2 and modeled foF2 by: IRI (black asterisk), IRImod (red dots), and IRI-Plas using Mg II (blue dots) for each of the selected stations, in terms of local time. The correlated series consist of monthly medians covering the period January 2008-December 2010.

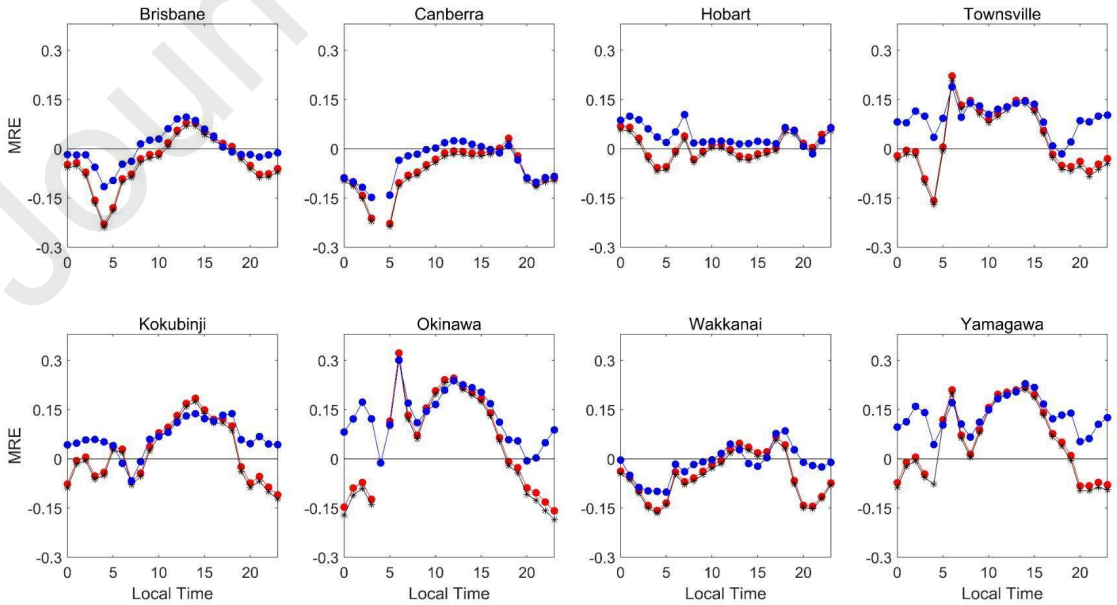

Journal Pre-proofs

Figure 9. Mean Relative Error (MRE) between observed foF2 and modeled foF2 by: IRI (black asterisk), IRImod (red dots), and IRI-Plas using Mg II (blue dots) for each of the selected stations, in terms of local time. The correlated series consist of monthly medians covering the period from January 2008-December 2010.

Another way of comparing foF2 modeled to observed data is through a dispersion diagram. Figs. 10 to 13 present the dispersion between modeled and observed foF2 values for Australian and Japanese stations, for each 3-year period separately, and also for nighttime and daytime local times, that is 8 different cases for each model. The nighttime cases include 23, 0, 1, and 2 LT, while the daytime cases include 11, 12, 13, and 14 LT. The linear fits between each model and observed time series are shown (dashed lines) together with the first bisector (solid black line) which correspond to perfect agreement. In most of the cases, the linear fits are very similar, which implies similar performance of the three models. The only difference can be noticed in the nighttime case during the minimum activity level period for both Australian and Japanese stations (Figs. 11 and 13, lower-right panels), where IRI-Plas outperforms the other two model options. In this case, the linear fit (blue dashed line) is closer to the bisector line than the other linear fits (black and red dashed lines).

In general, during high solar activity, the three IRI model estimations tend to overestimate the observed data for the lowest foF2 values and underestimate them for the highest values, as if the saturation effect is not completely solved by the model, being "over-considered" instead (Figs .10 and 12). During the minimum solar activity period, however, during daytime for the Australian (Fig. 11, upper panels), and Japanese (Fig. 13, upper panels) cases, there is an overall overestimation by the model across the entire foF2 range. It is also noteworthy that IRI and IRImod tend to underestimate foF2 values towards the lowest values during the Japanese, nighttime, low solar activity period (Fig. 13, left and middle lower panels).

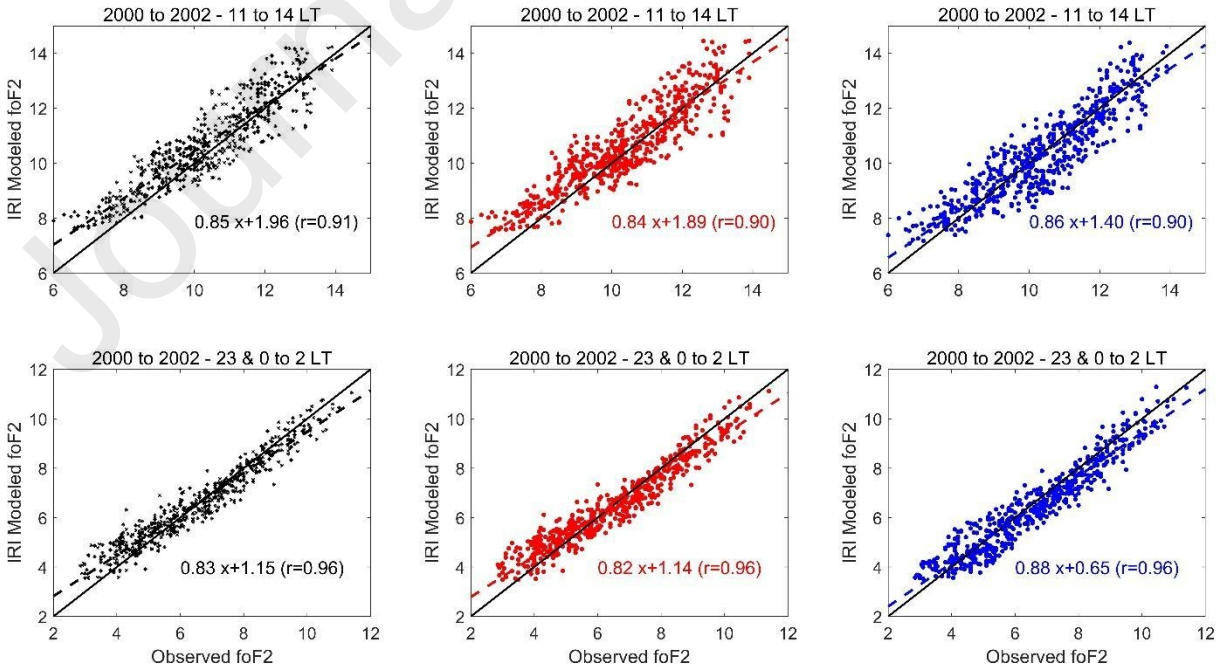

Figure 10. IRI modeled versus observed foF2 data considering the four Australian stations, 2000-2002 period: IRI (left panels, black asterisk), IRImod (middle panels, red dot) and IRI-Plas (right panels, blue dots). The black solid line represents the perfect fit between model and observed data. Dashed lines are the linear regression for each set of points. Upper panels: daytime hours (11 to 14 LT), lower panels: nighttime hours (23 & 0 to 2 LT). Linear regression fit equations with correlation coefficient indicated between brackets are indicated in the corresponding colors.

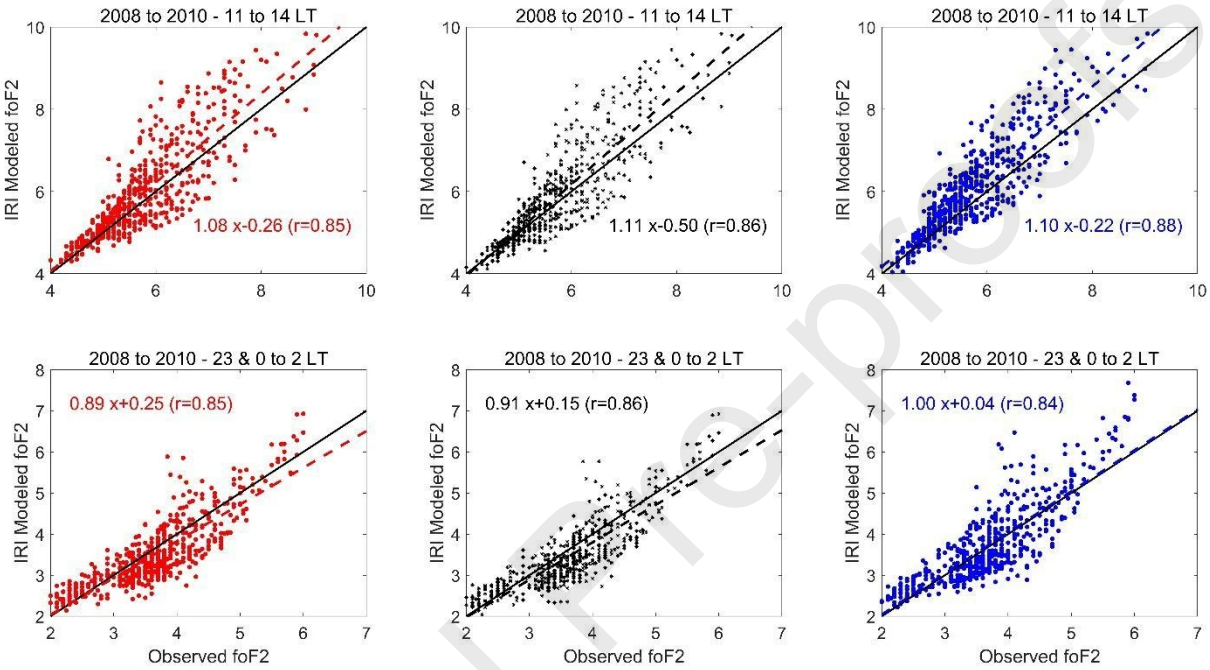

Figure 11. IRI modeled versus observed foF2 data considering the four Australian stations, 2008-2010 period: IRI (left panels, black asterisk), IRImod (middle panels, red dot) and IRI-Plas (right panels, blue dots). The black solid line represents the perfect fit between model and observed data. Dashed lines are the linear regression for each set of points. Upper panels: daytime hours (11 to 14 LT), lower panels: nighttime hours (23 & 0 to 2 LT). Linear regression fit equations with correlation coefficient indicated between brackets are indicated in the corresponding colors.

Journal Pre-proofs

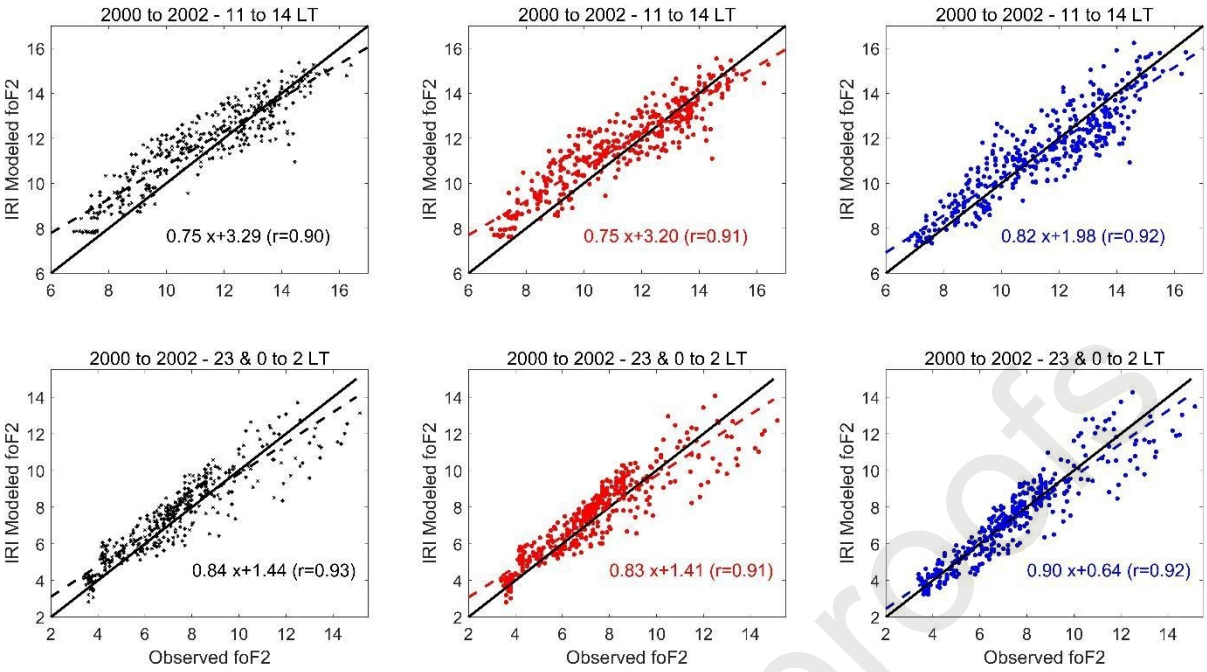

Figure 12. IRI modeled versus observed foF2 data considering the four Japanese stations, 2000-2002 period: IRI (left panels, black asterisk), IRImod (middle panels, red dot) and IRI-Plas (right panels, blue dots). The black solid line represents the perfect fit between model and observed data. Dashed lines are the linear regression for each set of points. Upper panels: daytime hours (11 to 14 LT), lower panels: nighttime hours (23 & 0 to 2 LT). Linear regression fit equations with correlation coefficient indicated between brackets are indicated in the corresponding colors.

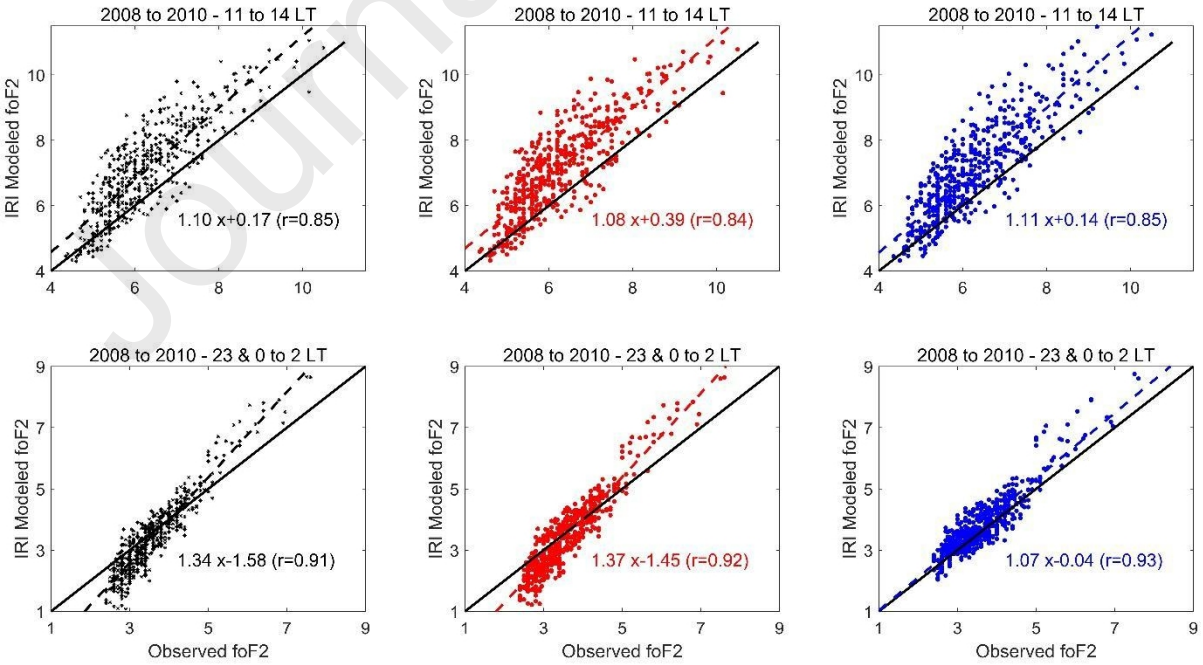

Journal Pre-proofs

Figure 13. IRI modeled versus observed foF2 data considering the four Japanese stations, 2008-2010 period: IRI (left panels, black asterisk), IRImod (middle panels, red dot) and IRI-Plas (right panels, blue dots). The black solid line represents the perfect fit between model and observed data. Dashed lines are the linear regression for each set of points. Upper panels: daytime hours (11 to 14 LT), lower panels: nighttime hours (23 & 0 to 2 LT). Linear regression fit equations with correlation coefficient indicated between brackets are indicated in the corresponding colors.

4. Discussion and conclusions

IRI-2016 performance modeling foF2 was assessed considering: (1) IG as a solar activity index in IRI-2016, that is the default option to model foF2 variation linked to solar activity variability, (2) Mg II instead of IG in IRI-2016; and (3) Mg II as a solar index in IRI-Plas model. Each model option was called: IRI, IRImod, and IRI-Plas, respectively. The comparison was made based on three statistical measures commonly used for this purpose: linear correlation (RHO), mean absolute error (MAE) and mean relative error (MRE), assessed between monthly medians along the 24 daily hours of foF2 assessed with each model option and foF2 measurements for eight ionospheric stations: four Australian and four Japanese stations. We considered two periods of three years around a maximum (2008-2010) and a minimum (2000-2002) solar activity level. Additionally, a visual inspection was also done through dispersion diagrams.

Based on RHO, MAE, and MRE figures, and also on mean values in Table 3, we conclude that the performance of the IRI-2016 model is not significantly improved by considering Mg II as a solar EUV proxy. Nor is the performance of IRI-Plas with the Mg II option. Moreover, we can make a rough comparison of the MAE mean values of Table 3 to the mean difference between IRI and IRImod foF2 estimations, and IRI and IRI-Plas foF2 estimations. For the periods 2000-2002 and 2008-2010 the differences resulted in 0.166 and 0.070 respectively in the IRImod case, and 0.490 and 0.320 in the IRI-Plas case. IRI-Plas presents greater differences with IRI-2016 than IRI-2016 modified with Mg II. However, the four values of mean differences just mentioned are around the same magnitude as MAE mean values between model and observation. This means that the model-observation difference is similar to the difference between the two IRI versions, and greater in some cases. This result provides an additional verification of the correct implementation of Mg II done by replacing the IG index in IRI-2016.

The dispersion diagrams show that the three models perform similar overall, with the same over and underestimation patterns except in the nighttime case during the minimum activity level period for both Australian and Japanese stations where IRI-Plas outperforms the other two model options.

In the comparative analysis of Abbas and Ameen (2022), they recognize the outperformance of Mg II, and recommend it as the index to be used for space weather modelling of foF2 at the stations they analyze in Pakistan and Japan, and even though the difference in the performances between F10.7, IG, Mg-II and Lyman-α, considering MAE for example, is stronger than ours, it does not exceed ~0.05 MHz on average.

One reason for observing negligible differences is that the stronger variation in the two periods considered is that corresponding to seasonality, which is not associated with solar EUV proxies. In fact, solar proxies do not present any seasonal variation. In addition, it seems that the increase in relative importance of the time variation due to specific forcings of each proxy is lower than foF2 seasonal

variation. Stronger differences should be noted considering statistical performance metrics applied to time series separated into local times and months (or season) along several years, or at least covering more than a solar activity fraction. The main variability will be linked then to solar activity variation. This option will be explored in the future adding also ionospheric stations covering wider regions.

Data availability

All ionospheric and indexes data are freely available in the following repositories: the Japanese stations' data from https://wdc.nict.go.jp/IONO/index_E.html; Australian stations from https://downloads.sws.bom.gov.au/wdc/iondata/au/; Mg II index is available from the University of Bremen at http://www.iup.uni-bremen.de/UVSAT/datasets/Mg II. The IRI-2016 model freely available in Fortran source code at https://irimodel.org/IRI-2016/; The IRI-Plas model used was obtained from its online version available at www.ionolab.org.

Competing interests

The authors declare that they have no conflict of interest.

Acknowledgments

B.S. Zossi, F.D. Medina, B.F. de Haro Barbas and A.G. Elias acknowledge research project PIP 2957. T. Duran acknowledge research projects PICT 2019-03491 and PGI 24/F083. M. Martínez-Ledesma acknowledges the support of ANID/FONDECYT Postdoctorado 3220581. M. Bravo acknowledges to ANID/FONDECYT Regular 1211144.

References

Abbas, F., M.A. Ameen (2022), Evaluation of ionospheric and solar proxy indices for IRI-Plas 2020 model over Pakistan and Japan during different solar activity epochs, Adv. Space Res, in press.

Arikan, F., Sezen, U., & Gulyaeva, T. L. (2019). Comparison of IRI-2016 F2 layer model parameters with ionosonde measurements. J. Geophys. Res., 124, 8092– 8109. https://doi.org/10.1029/2019JA027048

Bilitza, D., D. Altadill, V. Truhlik, V. Shubin, I. Galkin, B. Reinisch, and X. Huang (2017). International Reference Ionosphere 2016: From ionospheric climate to real-time weather predictions, Space Weather, 15, 418-429. https://doi.org/10.1002/2016SW001593

Bilitza, D., Pezzopane, M., Truhlik, V., Altadill, D., Reinisch, B. W., & Pignalberi, A. (2022). The International Reference Ionosphere model: A review and description of an ionospheric benchmark. Reviews of Geophysics, 60, e2022RG000792. https://doi.org/10.1029/2022RG000792

Brown, S., Bilitza, D., & Yiğit, E. (2018). Ionosonde-based indices for improved representation of solar cycle variation in the International Reference Ionosphere model. Journal of Atmospheric and Solar-Terrestrial Physics, 171, 137-146. https://doi.org/10.1016/j.jastp.2017.08.022

Bruevich, E. A., Bruevich, V. V., and Yakunina, G. V. (2014). Changed Relation between Solar 10.7-cm Radio Flux and some Activity Indices which describe the Radiation at Different Altitudes of Atmosphere during Cycles 21–23. Journal of Astrophysics & Astronomy, 35, 1-15. https://doi.org/10.1007/s12036-014-9258-0

Chicco D., Warrens M.J., Jurman G. (2021). The coefficient of determination R-squared is more informative than SMAPE, MAE, MAPE, MSE and RMSE in regression analysis evaluation. PeerJ Computer Science, 7, e623. https://doi.org/10.7717/peerj-cs.623

Clette, F., Svalgaard, L., Vaquero, J.M., Cliver, E.W. (2014). Revisiting the Sunspot Number. Space Science Reviews 186, 35–103 https://doi.org/10.1007/s11214-014-0074-2

Danilov, A.D., Konstantinova, A.V., (2023). Trends in foF2 to 2022 and various solar activity indices, Advances in Space Research, In Press. doi: https://doi.org/10.1016/j.asr.2023.01.028

Deminov, D.G., E.V. Nepomnyashchaya, V.N. Obridko, (2020). Solar activity indices for ionospheric parameters in the 23rd and 24th cycles. Geomagnetism and Aeronomy, 60 , 1-6. https://doi.org/10.1134/S0016793220010053

Elias, A. G., de Haro Barbas, B. F., Medina, F. D., and Zossi, B. S. (2021). On the Correlation between EUV Solar Radiation Proxies and their Long-Term Association, Proceedings of the Thirteenth Workshop "Solar Influences on the Magnetosphere, Ionosphere and Atmosphere", Bulgaria, 13-17 September 2021, edited by Katya Georgieva, Boian Kirov and Dimitar Danov, ISSN 2367-7570, pp. 20-23.

Erdem, E., and Arikan, F. (2017). IONOLAB-RAY: A wave propagation algorithm for anisotropic and inhomogeneous ionosphere. Turkish Journal of Electrical Engineering and Computer Sciences, 25, 1712–1723. https://doi.org/10.3906/elk-1602-119

Erturk, O., Arikan, F., & Arikan, O. (2009). Tomographic reconstruction of the ionospheric electron density as a function of space and time. Advances in Space Research, 43(11), 1702–1710. https://doi.org/10.1016/j.asr.2008.08.018

Gulyaeva, T.L., F. Arikan, I. Stanislawska (2011), Inter-hemispheric imaging of the ionosphere with the upgraded IRI-Plas model during the space weather storms, Earth Planets Space, 63 , 929-939. https://doi.org/10.5047/eps.2011.04.007

Gulyaeva, T., Arikan, F., Poustovalova, L., & Sezen, U. (2017). TEC proxy index of solar activity for the International Reference Ionosphere IRI and its extension to Plasmasphere IRI-Plas model. International Journal of Scientific Engineering and Applied Science (IJSEAS), 3(5), 144–150.

Gulyaeva, T.L., F. Arikan, U. Sezen, L.V. Poustovalova (2018), Eight proxy indices of solar activity for the International Reference Ionosphere and Plasmasphere model, Journal of Atmospheric and Solar-Terrestrial Physics, 172, 122-128. https://doi.org/10.1016/j.jastp.2018.03.025

Lastovicka, J., A.V. Mikhailov, T. Ulich, J. Bremer, A.G. Elias, N. Ortiz de Adler, V. Jara, R. (2006). Abarca del Rio, A.J. Foppiano, E. Ovalle, A.D. Danilov, Long-term trends in foF2: A comparison of various methods, Journal of Atmospheric and Solar-Terrestrial Physics, 68, 1854-1870. https://doi.org/10.1016/j.jastp.2006.02.009

Lastovicka, J., (2021a). What is the optimum solar proxy for long-term ionospheric investigations?, Advances in Space Research, 67, 2-8. https://doi.org/10.1016/j.asr.2020.07.025

Lastovicka, J., (2021b). The best solar activity proxy for long-term ionospheric investigations. Advances in Space Research, 68, 2354-2360. https://doi.org/10.1016/j.asr.2021.06.032

Liu, R., Smith, P., & King, J. (1983). A new solar index which leads to improved foF2 predictions using the CCIR Atlas. Telecommunication Journal, 50, 408–414.

Liu, L., W. Wan, Y. Chen, & H. Le (2011). Solar activity effects of the ionosphere: A brief review,

Chinese Science Bulletin, 56, 1202−1211, doi: 10.1007/s11434-010-4226-9.

Liu, Z., Fang, H., Weng, L., Wang, S., Niu, J., & Meng, X. (2019). A Comparison of Ionosonde Measured foF2 and IRI-2016 Predictions Over China. Adv. Space Res., 63, 1926-1936. doi:10.1016/j.asr.2019.01.017

Maltseva, O. A., & Poltavsky, O. S. (2009). Evaluation of the IRI model for the European region. Advances in Space Research, 43(11), 1638–1643. doi:10.1016/j.asr.2008.08.019

Mielich, J., J. Bremer, (2013). Long-term trends in the ionospheric F2-region with different solar activity indices. Annales Geophysicae, 31, 291-303. https://doi.org/10.5194/angeo-31-291-2013

Sezen, U., Sahin, O., Arikan, F., & Arikan, O. (2013). Estimation of hmF2 and foF2 communication parameters of ionosphere F2-layer using GPS data and IRI-Plas model. IEEE Transactions on Antennas and Propagation, 61(10), 5264–5273. https://doi.org/10.1109/ TAP.2013.2275153

Sezen, U., Gulyaeva, T. L., & Arikan, F. (2018). Performance of solar proxy options of IRI-Plas model for equinox seasons. J. Geophys. Res., 123, 1441– 1456. https://doi.org/10.1002/2017JA024994

Snow, M., M. Weber, J. Machol, R. Viereck, and E. Richard (2014). Comparison of Magnesium II core-to-wing ratio observations during solar minimum 23/24, Journal of Space Weather and Space Climate, 4, A04. https://doi.org/10.1051/swsc/2014001

Tsagouri, I., Goncharenko, L., Shim, J. S., Belehaki, A., Buresova, D., & Kuznetsova, M. M. (2018). Assessment of current capabilities in modeling the ionospheric climatology for space weather applications: foF2 and hmF2. Space Weather, 16, 1930– 1945. https://doi.org/10.1029/2018SW002035

Tuna, H., Arikan, O., Arikan, F., Gulyaeva, T. L., & Sezen, U. (2014). Online user-friendly slant total electron content computation from IRI-Plas: IRI-Plas-STEC. Space Weather, 12, 64–75. https://doi.org/10.1002/2013SW000998

Viereck, R. A., M. Snow, M. T. DeLand, M. Weber, L. Puga, and D. Bouwer (2010). Trends in solar UV and EUV irradiance: An update to the Mg II Index and a comparison of proxies and data to evaluate trends of the last 11-year solar cycle, Abstract GC21B-0877 presented at 2010 Fall Meeting, AGU, San Francisco, CA, 13-17 Dec.

Willmott, C.J., Matsuura, K., (2005). Advantages of the mean absolute error (MAE) over the root mean square error (RMSE) in assessing average model performance. Climate Research, 30, 79–82. https://doi.org/10.3354/cr030079

Journal Pre-proofs

Declaration of Interest statement:

The authors declare that they have no conflict of interest.

Journal Pre-proofs